



Delimitation of the Pore in Tweety Homolog 1 Channels: A Model-guided Approach

J. P. Reyes^{1*}, J. R. Castillo-Hernández¹, M. I. Maldonado-Cervantes¹,
E. Maldonado-Cervantes¹, A. Rangel López², A. A. Vértiz Hernández²
and M. García-Rangel¹

¹Laboratorio de Biomedicina, Unidad Académica Multidisciplinaria Zona Media, Universidad Autónoma de San Luis Potosí, Carretera Rioverde-San Ciro, Km. 4, Rioverde, S.L.P., 79617, Mexico.

²Área de Enfermería, Coordinación Académica Región Altiplano, Universidad Autónoma de San Luis Potosí, Carretera Central Km 6, Matehuala, S.L.P., 78700, Mexico.

Authors' contributions

This work was carried out in collaboration between all authors. Author JPR conceived and designed the study, performed part of the experiments and modeling, wrote the study protocol, and also wrote the draft of the manuscript. Authors JRCH and MIMC participated in modeling, participated in manuscript elaboration, and they also technically attended the performance of the experimental protocol of this study. Authors EMC, ARL and AAVH performed part of the experiments and modeling. Author MGR performed the statistical analysis of the study, and participated in fitting of the data, and management of literature searches. All authors read and approved the final manuscript.

Article Information

DOI: 10.9734/JABB/2016/29145

Editor(s):

(1) Anil Kumar, Professor & Head (Chair), School of Biotechnology, Devi Ahilya University, Madhya Pradesh, India.

Reviewers:

(1) Valentina Gatta, University of Chieti, Italy.

(2) Asita Elengoe, Universiti Teknologi Malaysia, Malaysia.

(3) Zarrin Basharat, Fatima Jinnah Women University, Pakistan.

Complete Peer review History: <http://www.sciencedomain.org/review-history/16648>

Original Research Article

Received 25th August 2016
Accepted 8th October 2016
Published 25th October 2016

ABSTRACT

Tweety homolog proteins have been indicated as 'putative anion channels', but yet there is some lack of definitive data in this regard. Here, we focused on the human Tweety homolog 1 protein (hTTYH1), and elaborated a model based on residue-coevolution analysis and *ab initio* principles. This much satisfactory model, was tested through sited-directed mutagenesis of residues, R371 and F394. Mutation of these residues resulted in alterations in ion selectivity and blocker sensitivity, respectively, confirming the predictions from the model. Hence, our results strengthen the idea that these proteins are in fact anion channels. As well, our model can be used to propose further structure-function relationships. Similar approaches can be employed for other channels, which

*Corresponding author: E-mail: pablo.reyes@uaslp.mx;

have unknown structure, due to the very technically demanding and sometimes uncertain process of crystallization of membrane proteins for X-ray crystallography.

Keywords: *Tweety homolog; anion channel pore; site-directed mutagenesis.*

1. INTRODUCTION

Knowledge of the structure of proteins may be a crucial factor in understanding their function. Besides, this knowledge can be important to understand some physiological or pathological conditions. Unfortunately, membrane proteins and ion channels have proven particularly difficult regarding determination of their structure; in most cases, isolation from the membrane lipid environment prevents them from crystallization in a native or nearly-native conformation, and dedicated work and special strategies are necessary for success [1]. This is reflected in the fact that even though membrane proteins roughly represent the 22% of all proteins, and have remarkable importance as therapeutic targets, they only account for about 2.5% of known structures deposited in the Protein Data Bank [2]. In view of this problem, much effort, time, and computer resources have been invested in the development of software aimed at providing models of membrane proteins with unknown structure [3]. It is clear that currently there is much emphasis in the improvement of structure predictions for membrane proteins, and fields to account for the membrane environment are frequently revised, improved and optimized, in new implementations of prediction software. Accurate membrane fields are particularly important in the *ab initio* approaches, such as the ones implemented by Rosetta and the Biochemical Library (BCL) [4]. In cases where homology modeling or threading are not of much help, an approach based on residue coevolution can be a good complement to *ab initio* approaches, and in fact *ab initio* implementations (Rosetta, BCL) allow for the imposition of contact restraints [2]. Residue coevolution analysis allows the identification of pairs of residues that are likely to be in contact in the membrane protein native structure [5]; these can be imposed as contact restraints during modeling. In our present work, we employed residue coevolution analysis for the identification of residue pairs likely to be in contact within the transmembrane domains of tweety homolog 1 protein. Subsequent geometrical criteria and lipid exposition analysis criteria were used to further enrich the initial selection, keeping the most likely contact pairs. Finally, BCL membrane (transmembrane domains) *ab initio* runs with

contact restraints [4], were used to obtain the best model (i.e., the one with the lowest energy and the most contacts still in place).

The tweety homolog 1 protein (TTYH1) is still enigmatic in different aspects. It belongs to a family of tweety homologs, TTYH 1-3 [6]. There is considerable evidence that members of this family constitute chloride channels [7,8]. However, this early evidence is taken somewhat cautiously, and these proteins are usually referred to as 'putative' chloride channels [9-12]. Their structure is unknown, as well as the stoichiometry of the putative channel. Nevertheless, bioinformatics and experimental glycosylation studies indicate that these membrane protein subunits possess five transmembrane domains [10]. Interestingly, overexpression of proteins of this family has been observed in cases of different tumors [13, 14], even though no clear mechanism suggesting a causal role in tumorigenesis has been disclosed by the moment. This resembles the case of TMEM16A (Anoctamin 1) chloride channels, except that in this latter case there is more evidence of a direct causal role of TMEM16A in tumorigenesis [15,16]. Moreover, other remarkable resemblance is that both TMEM16A and TTYH3 are claimed to be anion channels activated by an increase in cytosolic calcium (calcium-activated chloride channels or CaCC) [17]; this is seemingly different from TTYH1, which instead is claimed to be swelling-activated [8]. Remarkably, it has been proposed that TTYH proteins may have a similar structure to the high-conductance calcium-activated potassium channels (BK_{Ca} or Maxi K⁺ channels), which is supported by the presence of an intracellular aspartate-rich region in both types of channels, past the carboxyl terminus of the last pore-forming transmembrane domain [7,8]. In the case of the BK_{Ca} channels this region makes a fundamental contribution to the well-known 'calcium bowl', and it is proposed that a similar structure in TTYH proteins might regulate calcium sensitivity, including the activation by calcium of the TTYH3 maxi Cl⁻ channels [7].

In the present work, we elaborate a structural model of TTYH1, based on residue coevolution analysis, geometrical and lipid exposition restraints, and *ab initio* Monte-Carlo energy

optimization, which we think that is likely to be close to the real native structure. From the tertiary structure of the model, we make inferences about its possible quaternary structure, finding that a tetrameric assembly is likely. A tetrameric assembly, with the fifth transmembrane domain (TM5) involved in pore formation, much resembles the structure of BK_{Ca}; thus giving further support to the initial proposal of a structural similarity between these Maxi K⁺ and Maxi Cl⁻ channels. We subjected our model to empirical test, and our experimental results are pretty consistent with the predicted disposition of the pore, according to the model.

2. MATERIALS AND METHODS

2.1 Clones, Cells and Transfection

The hTTYH1 clone was purchased from Origene (Rockville, MD, USA), and sequenced at Biotechnology Facility of the National Autonomous University of Mexico, UNAM. Its sequence completely agreed with that deposited in the GeneBank (Accession NP_065710; 450 residues). Site-directed mutagenesis was carried out by means of the QuikChangeLightning site-directed mutagenesis kit (Agilent Technology), following the manufacturer's instructions, as usually done in our previous research [18,19]. Successful achievement of the R371Q and F394S mutations was verified by sequencing. For expression in the human embryonic kidney 293 cell line (HEK-293 cells), the sequences were cloned into the pIRES2-EGFP vector. HEK-293 cells, maintained in DMEM (Gibco) with 10% fetal bovine serum at 37°C, oxygen supplied along with 5% CO₂, were transfected using the Lipofectamine 2000 transfection reagent (Invitrogen) and plated on glass coverslips coated with poly-L-lysine.

2.2 Recordings and Solutions

Cells in the glass coverslips were placed in a recording chamber mounted on the stage of an inverted microscope (Olympus CKX41, Melville, NY, USA) equipped with UV illumination. External solutions were gravity-perfused into the recording chamber at a flow rate of 2 ml/min. Whole-cell currents were recorded from individual transfected cells using the Patch-Clamp Whole-Cell configuration. Recordings were performed with the Axopatch 200B amplifier (Molecular Devices) interfaced to a Digidata 1200 using a pClamp v8 for recording and analysis (Molecular Devices). Analog signals

were acquired and filtered at 1 kHz. Patch pipettes (Sutter Instruments, Novato, CA, USA) were fabricated with borosilicate glass capillaries using a four-step horizontal Flaming–Brown microelectrode puller (Sutter Instruments) and had resistances of 3.5–5 MΩ when filled with internal pipette solution. The pipette (internal) solution contained (in mM): NaCl 140.0, MgCl₂ 1.0, HEPES 5.0 (pH=7.2). The external bath solution contained (in mM): NaCl 140.0, CaCl₂ 1.0, MgCl₂ 1.0, HEPES 5.0 (pH=7.3; 282 mOsm). The external hypotonic solution used to stimulate (swelling stimulus) contained (in mM): NaCl 100.0, CaCl₂ 1.0, MgCl₂ 1.0, HEPES 5.0 (pH=7.3; 207 mOsm). The stimulus that combined swelling and intracellular Ca²⁺ increase ('swelling+Ca²⁺') was applied by perfusion into the recording chamber of external hypotonic solution supplemented with 1 μM ionomycin. Upon the beginning of the stimulus (either 'swelling' or 'swelling+Ca²⁺' stimulation), at least five minutes were allowed to elapse in order to obtain robust development of currents in the presence of the stimulus, and then different voltage protocols were applied. All measurements done in the preparation of Fig. 4 were made with a 'swelling+Ca²⁺' stimulus, and after at least five minutes from the beginning of this stimulation. For the experiments that are shown in Fig. 4A, different external solutions which had 35, 70, 100, 140, 200, and 350 mM NaCl were applied, and the respective reversal potential measured. All other components of these external solutions remained the same, with the exception that in those with the lower concentrations of NaCl, D-mannitol was added in order to attain an osmolarity of about 207 mOsm. Voltage ramps (from -100 mV to +100 mV; 150 ms long; every 2 s) were applied for the experiments shown in Fig. 3E and all the experiments in Fig. 4. Dose-response curves for 4,4'-diisothiocyano-2,2'-stilbene-disulfonic acid (DIDS) blockage at different voltages, were prepared from voltage ramps as described elsewhere [18]. DIDS (from a DMSO stock solution) was applied to the cells at final concentrations in the external solution of 0.1, 1, 5, 10, 50, 100 and 300 μM.

2.3 Structural Modeling of the hTTYH1 Protein

Prediction of membrane protein structure can proceed through different strategies. For proteins with a considerable degree of homology to other protein(s) of known structure, a homology modeling approach can be applied; or a

threading approach in case of more distantly related proteins. When those approaches are not possible, due to the lack of proteins with known structure which could guide the prediction for the target protein, then an *ab-initio* approach (physical first principles) can be a very successful and insightful one. In particular, combination of *ab initio* modeling with contact restraints is a very powerful strategy to obtain good models, close to the native structure of proteins with known structures thus far tested.

Residue Coevolution Analysis exploits the fact that pairs of residues which are in contact in the tridimensional structure of a protein, and are important to keep this structure and/or its function, change or mutate in a correlated manner. This analysis is carried out with a number high enough of related protein sequences, in a multiple sequence alignment, taking advantage of the recent boom in sequencing facilities and available sequence data. Besides, remarkable advances in the mathematical processing of the data have been made recently in order to reduce the appearance of 'indirect couplings' (i.e., false positives), that could obscure the analysis and its results. Only the contacts between TM domains of hTTYH1 were considered. Contacts with high likelihood of being involved in relevant structural and functional scaffolds and to coevolve, were obtained as described elsewhere [20-22]. The reputed online server EVfold (Hopf et al. 2014a) was mainly used, with default settings, which have proven to yield good results for other proteins alike. In addition, other Direct Coupling Analysis (DCA) software run in MATLAB (Morcos et al. 2014) gave very similar results, denoting the consistency/robustness of the contacts obtained as a result.

The top 50 highly scored contacts were employed as contact restraints in *ab initio* modeling. The Biochemical Library (BCL; Meiler Lab, Vanderbilt University) was used for this purpose [2,4]. This Library depends on the Monte Carlo method, a complete, advanced and sophisticated scoring function, and moves in the membrane plane, taking into account particularly designed membrane fields; the parameters were set as recommended by the BCL developers in order to yield optimal results [2]. Only the TM domains were built and represented in the PDB files used by BCL. A total of 900 different models were produced. From these 900 models, the ones with the minimal energy values (i.e., supposedly close to the native conformation)

were carefully analyzed. In addition, the number of contacts preserved in the structures was obtained for each of the 900 models. It was observed that the models with the maximal number of contacts preserved were also among the ones with the minimum energy, which is in favor of a great closeness between the model and the real structure.

Once the final model of one channel subunit was obtained, we used the ZDOCK Online Server software [23]. In particular, in order to determine the most likely number of subunits and the relative positions between each, we used M-ZDOCK on this server [23]. To our delight, we observed that a tetrameric assembly is the more likely, and that the TM5 domains seem to be the most important in pore conformation. In order to get to this conclusion, we compared the normalized scores arising from the different subunit stoichiometries, where trimeric, tetrameric and pentameric subunit conformations clearly outperformed other stoichiometries, but the tetrameric conformation yet much significantly stood as the best one, over the trimeric and pentameric ones. All these conformations displayed TM5 domains organized around the putative central pore cavity, as shown in Fig. 2.

2.4 Fitting and Data Analysis

The Goldman-Hodgkin-Katz equation was used to fit data points in Fig. 4A, where P_{Na}/P_{Cl} was left as a free parameter.

Voltage dependence of the blockage (Figs. 4C, D, and E) was assessed using voltage ramps by calculating the following ratio: $I_{B=x}/I_{B=0}$, where $I_{B=x}$ is the current with settled effect of DIDS at any given 'x' concentration, and $I_{B=0}$ is the control maximum current (i.e., the concentration of blocker equals zero). By varying the concentration, 'x', of blocker, a family of $I_{B=x}/I_{B=0}$ curves was obtained. Data were then plotted (by transposing blocker concentration and voltage) in order to construct the family of 'unblocked fraction-dose' curves, where each curve corresponds to a specific, selected membrane voltage. The curves of unblocked fraction as a function of blocker concentration were then fit by a Hill equation:

$$\frac{I}{I_{B=0}} = \frac{I_{min}}{I_{B=0}} + \frac{1 - \frac{I_{min}}{I_{B=0}}}{1 + \left(\frac{[B]}{K_d}\right)^{n_H}}$$

Where I is the current in the presence of a given concentration of blocker ($[B]$), $I_{B=0}$ is the maximum current in the absence of blocker, I_{min} is the current obtained at saturating concentrations of blocker, $I/I_{B=0}$ is the unblocked fraction (which goes from 1 (no block) to $I_{min}/I_{B=0}$ (maximum effect)), K_d is the concentration of blocker at which half-maximal effect is attained, and n_H is the Hill number. The K_d values obtained from the fits were plotted as a function of the corresponding voltage (depicted in Fig. 4F). A Woodhull analysis [24] was then performed for the resulting curve:

$$\log(K_d(V)) = \log(K_d(0)) + \delta z F V / 2.303 RT$$

Where δ is the electrical distance of block, V the membrane voltage, $K_d(V)$ is the value of K_d at the specified voltage, $K_d(0)$ is the value of K_d at 0 mV, and z , F , R , T have their usual thermodynamic meanings. Thus, the value of δ was derived from the fits of the K_d vs. V plots, which allowed us to determine the value of the $\delta z F V / 2.303 RT$ term, and from it to calculate δ .

The two-tailed Students t -test for unpaired samples was used to evaluate the significance of differences between experimental group means ($P < 0.05$). Data are expressed as the mean \pm SEM; N indicates the number of cells tested.

3. RESULTS

The first part of our study was a modeling approach. It is known that TM domain packing is a major thermodynamic factor that makes a very significant contribution to the overall energetics of native membrane protein conformation [25]. Thus, we particularly focused in identifying pairs of contacts between TM domains that are the most likely, according to the most recent advances aimed to achieve this goal. After that, we run *ab initio* Monte-Carlo modeling of the TM domains only, with contact restraints included, to fulfill both requirements of minimum energy at the native conformation, while trying to keep the more possible contacts. To our delight, we observed that a very good model in terms of minimal energy (at the very same level of the minimum energy one without contact restraints) was feasible while keeping most of identified contacts; this points to a model that is highly likely to be close to the real native conformation of the protein. Fig. 1 shows the best model obtained, with a very good correspondence between minimum energy and contact preservation.

After having obtained a subunit of the channel as described, we carried out docking, with variable number of subunits, in order to explore which quaternary structure would be most favored. Again, to our delight – taking into account that TTYH channels have been likened to tetrameric BKCa channels - we observed that a tetramer of such subunits was the most energetically favorable quaternary structure. Fig. 2 depicts the best quaternary structure that was obtained through this procedure. Among our 50 highly-scored contacts obtained, we observed that a good share of them are justified as very likely inter-subunit contacts, again supporting a likely model.

After obtaining the model, we experimentally tested hTTYH1 function as an ion channel. First, we made a characterization of the behavior of hTTYH1 expressed in HEK-293 cells, in our experimental setup. We observed that upon expression of this protein, there is an additional component of swelling-activated current, which is not observed in mock cells.

It has previously been reported that hTTYH3 is a calcium-activated anion channel, while hTTYH1 is instead a swelling-activated anion channel. This is the reason why, in a first instance, we stimulated with hypotonic external medium. Nevertheless, even though we observed responses upon this stimulation alone, we noticed that there was a considerable variability in the response amplitudes, yet significantly different from the control (Fig. 3F), indicating that current activation proceeds somewhat inconsistently from cell to cell. However, this variability was much greatly diminished, leading to high amplitude and more homogeneous responses when the swelling stimulus was accompanied by ionomycin, an agent that induces an increase in cytosolic Ca^{2+} (Fig. 3F). This suggests that hTTYH1 may have a component of calcium sensitivity too; maybe a latent one which manifests upon its main activation through swelling. Thus, expression of hTTYH1 determined that upon stimulation with swelling and ionomycin, the current was consistently and significantly activated with a faster slope and to higher amplitude (Figs. 3A and B). It is then clear that expression of hTTYH1 results in an extra current that is likely to be mediated by the hTTYH1 proteins working as anion channels, as has been previously reported [7,8].

When voltage steps and ramps were applied, the hTTYH3-induced swelling and calcium-activated

current appeared as quite linear, with no apparent voltage dependence (Figs. 3C and D). In the I-V curves, this linear behavior was broken when DIDS was applied, as this blocker mainly exerted its effect on the outward current without affecting the inward current, in a voltage dependent fashion. As shown in Fig. 3E, in hTTYH1-expressing cells, the amplitude of the response is dramatically reduced in the presence of DIDS, which indicates that this is an anion current, as has been previously reported (see also Fig. 4).

Having characterized hTTYH1 in its WT form, we studied mutants of this protein in order to investigate whether our structural predictions based on the model could hold. First, we studied the relative permeabilities of Na⁺ and Cl⁻ (P_{Na}/P_{Cl}) and observed that the mutant R371Q behaved differently from the WT, while the mutant F394S was undistinguishable from the WT. This is consistent with the report by Suzuki and Mizuno [8], where mutation of the homologous residue in hTTYH3 results in a similar alteration in channel permeability. However, when studying the voltage dependence of DIDS block, we observed the somewhat opposite scenario that mutation R371Q did not affect DIDS blockade, while mutation F394S had an important effect on DIDS blockade. Thus, these results indicate that both mutated residues have important, but different, influences on hTTYH1; while R371Q affects ion permeability, F394S affects blocker binding. These results support our structural predictions based on modeling, as will be discussed in the following.

4. DISCUSSION

TTYH family channel proteins have remained somewhat unexplored. Even though it has been reported that expression of TTYH proteins gives rise to anion conductances and that mutation in hTTYH3 result in perturbations of some biophysical properties of these conductances - thus indicating bona-fide ion channels - [7,8], these early findings seem to have been taken cautiously, and a number of authors have opted to refer to these proteins as 'putative ion channels' [10].

Here we present the results of a modeling approach, which are consistent with a protein where the several subunits – likely four of them – contribute to the pore through their TM5 transmembrane domain. The model obtained is highly likely, because it best accommodates evolutionary contact restraints, protein energy

minimization and access area exposed. According to docking energetic considerations, the protein is most likely a tetramer. Having in mind that it has been proposed that TTYH channels may have structural similarities with BKCa channels [8], and that in fact it is known that calcium-activated anion and BKCa channels share a common pharmacology [26], the tetrameric assembly herein suggested by our modeling approach gives further support to these structural similarities previously exposed.

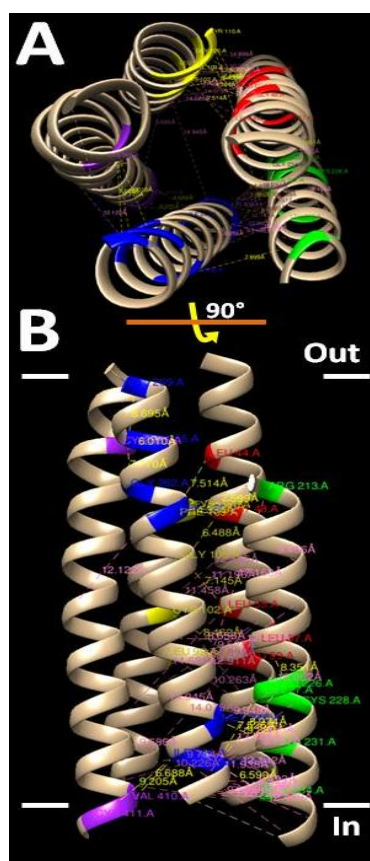


Fig. 1. Predicted tertiary structure of hTTYH1
Best model - out of 900 models generated - obtained of hTTYH1 channel subunit protein. See Materials and Methods for more details. Some of the most highly scored contacts predicted by residue coevolution analysis, are shown as completely feasible in the structure, and the good overall compagination of contacts among helical faces, strengthens the model as highly likely. Critical residues involved in contacts are shown in different colors. Residues in TM1 are in red, in TM2 in yellow, in TM3 in green, in TM4 in blue, and in TM5 in purple. The subunit is placed in the same position as in Fig. 2, for the ease of comparison. (A) Top, extracellular side, view. (B) Lateral view, immersed in the membrane (white lines represent the outer and inner membrane surfaces within which the TM domains span)

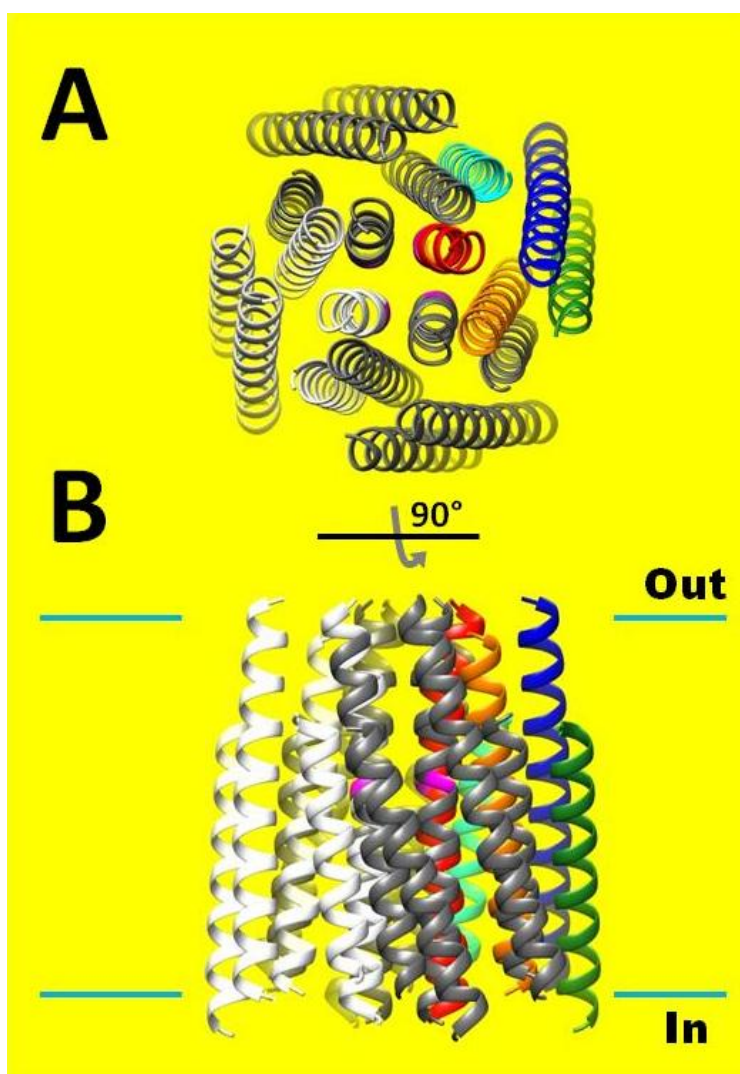


Fig. 2. Predicted quaternary structure of hTTYH1

With the structural model of a hTTYH1 channel subunit shown in Fig. 1, we carried out docking studies, involving different number of identical subunits in each case. The best result is depicted; we found that a tetrameric assembly was the one that was best suited, giving a very good and coherent structure. See Materials and Methods for more details. One of the subunits (in the same position as in Fig. 1) is shown in different colors (TM5 in red), the other subunits are shown in different shades of gray. (A) Top, extracellular side, view. (B) Lateral view, immersed in the membrane. Cyan lines represent the outer and inner membrane surfaces within which the TM domains span. Note that the putative pore is mainly contributed by TM5. The current structure likely corresponds to a closed state of the channel. The residue F394 is colored in magenta in each subunit, about half way across the membrane

Furthermore, as shown in Fig. 5, past the carboxyl terminus of TM5 and in the intracellular medium, there is an Aspartate-rich region which could conform a Ca^{2+} -binding structure resembling the 'Ca²⁺ bowl' of BKCa. The hTTYH1 channel studied here, though not strictly a calcium-activated channel, seems to have calcium sensitivity upon primary activation by a swelling stimulus. Thus, calcium sensitivity –

likely mediated by this putative Ca^{2+} -binding site – may be more widespread among TTYH family proteins than previously thought. We propose that swelling and Ca^{2+} may contribute to lead to the open state of the hTTYH1 channels (this is represented in Fig. 5, with arrows representing some possible outward gating motions of TM5 domains).

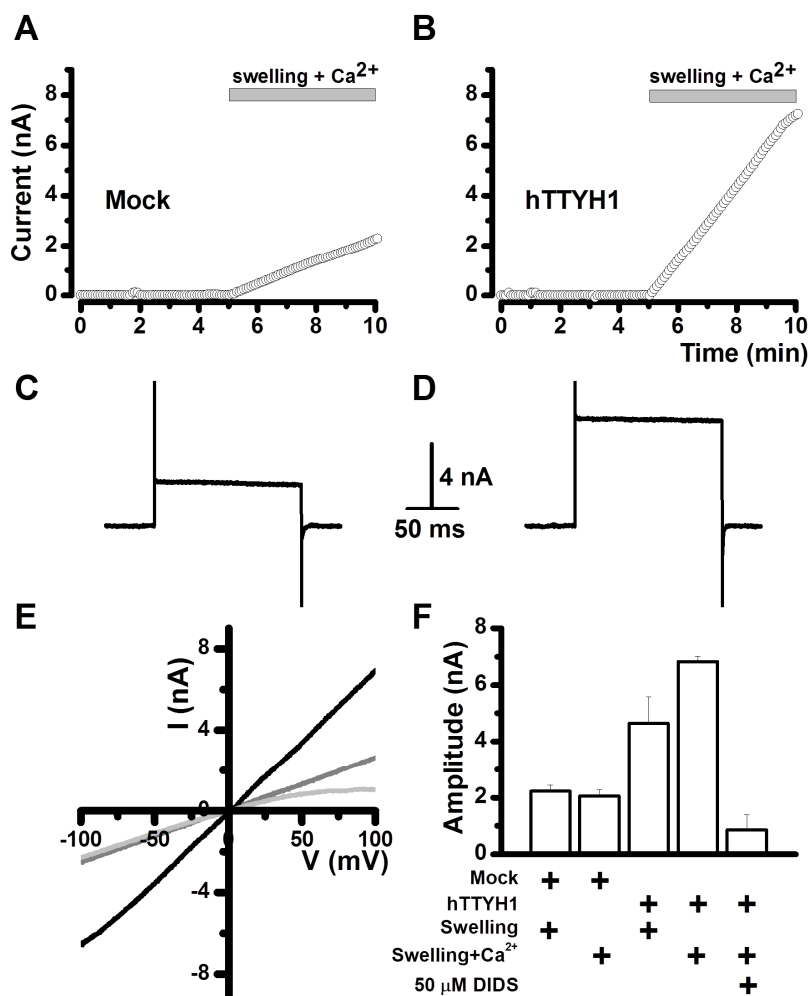


Fig. 3. Expression of hTTYH1 induces a current activated by swelling and possibly assisted by Ca²⁺

(A and B) Stimulation with a hypotonic external medium (swelling stimulus) results in a relatively modest activation of current in mock-transfected cells (A), but current activation has a larger slope and reaches much higher amplitude in hTTYH1-transfected cells upon the same stimulation (B). (C and D) Upon activation of the current with swelling+Ca²⁺ stimulation, the response to a +100 mV voltage step is shown. As expected, in mock-transfected cells (C), the current amplitude is smaller than in hTTYH1-transfected cells (D). Nevertheless, the current in both cases is nearly flat, with no apparent voltage-dependent component. (E) Current-voltage (I-V) relationships for mock-transfected cells (gray trace), hTTYH1-transfected cells (black trace), and hTTYH1-transfected cells exposed to 50 μM DIDS (light gray trace). Note that DIDS mainly blocks the outward current, in a voltage-dependent manner. (F) Current amplitudes obtained in different conditions, as indicated. Note that in mock-transfected cells there is no difference between swelling and 'swelling+Ca²⁺' stimulation, while in hTTYH1-transfected cells the response to swelling alone tends to be significantly smaller and with more variability than the response to 'swelling+Ca²⁺'. N=9 in all cases

The selectivity filter in BKCa channels is very likely to be at the extracellular side of the pore, and to be constituted by transmembrane segments S5, S6, and remarkably by the loop linking S5 and S6 [27]. Similarly, and according to our model and also to a previous data [8], the selectivity filter in hTTYH1 channels is likely to be

located at the extracellular side of the pore, mostly determined by TM5 and the loop linking TM4 and TM5 (see Fig. 5). In fact, in hTTYH3, it has already been shown that mutation of a positively-charged residue in the TM4-TM5 loop (close to the N-terminus of TM5), Arginine 366 to Glutamine, results in a pore more permeable to

cations, i.e. P_{Na}/P_{Cl} increased [8]. Because our model is generally concordant with this previous proposal [7] and since mutation of the homologous residue in hTTYH1 had not been done, we tested the R371Q mutation in hTTYH1, which is homologous to R366Q in hTTYH3. As expected, we observed an important increase in P_{Na}/P_{Cl} (see Fig. 4B), which most likely indicates that hTTYH1 and hTTYH3 have a

similar structure, and that TM5 forms part of the pore wall, while the TM4-TM5 loop contains at least a residue that belongs to the selectivity filter of the channel. This is represented in Fig. 5, with a chloride ion influenced by the positively-charged R371 residues, thus providing an electrostatic basis for the selectivity filter preferring anions over cations in the WT protein.

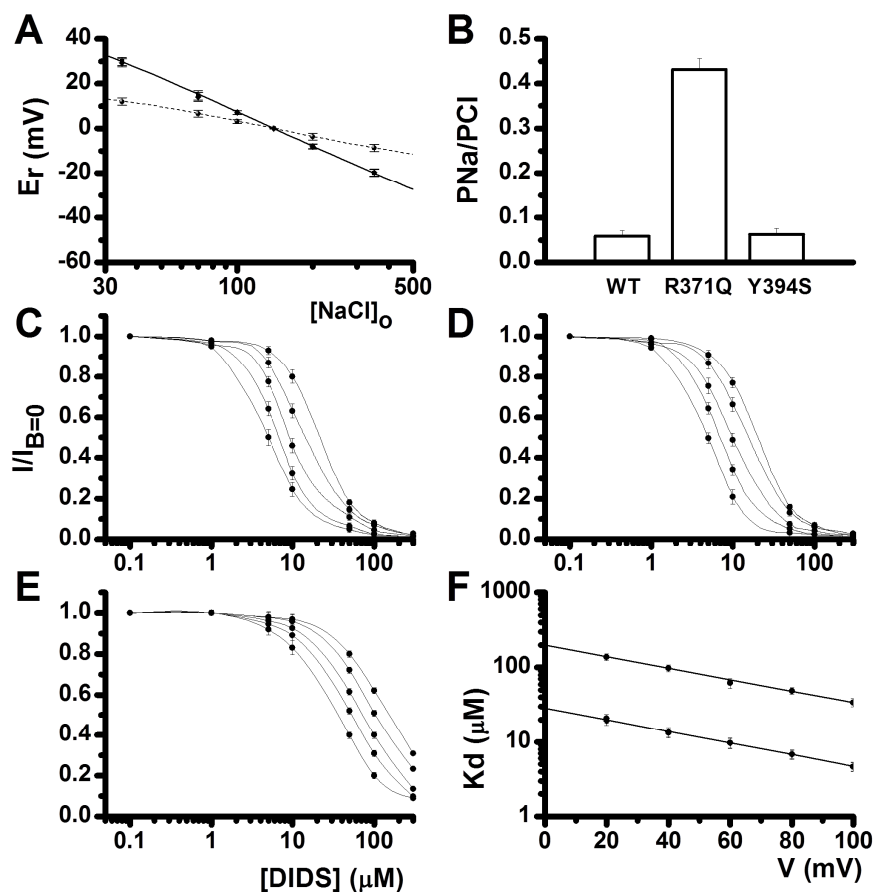


Fig. 4. Mutations in residues pointed by the model to be located in functionally critical positions

A.- Mutation of R371 at the external mouth of the pore results in a drastic change in anion/cation selectivity, towards an increase in cation permeability (dashed line; diminished reversal potential values at all $[NaCl]_o$ values indicate increased cation permeability). Experiments were carried out changing the external $[NaCl]$ and measuring the resulting reversal potential. Continuous lines are fits to the GHK equation for WT and F394S, while dashed line is the corresponding fit for R371Q. From these curves, the P_{Na}/P_{Cl} ratios were obtained. See Methods for more details. **(B)** Summary of P_{Na}/P_{Cl} ratios obtained from experiments as in **(A)**. **(C and D)** Dose-response curves for DIDS blockade at different voltages. Each continuous line is the fit of the Hill equation for a specific voltage value (from +20 mV to +100 mV in 20 mV steps). From these fits, the respective K_d values were obtained. Curves are shown for WT **(C)** R371Q **(D)**, and F394S **(E)** hTTYH1 proteins. **(F)** Curve of K_d vs membrane potential for WT, R371Q and F394S proteins. Note that the K_d values for the F394S mutant are significantly higher than those of the WT or R371Q, but the slope – which is related to the electrical distance of block – did not change. See Methods for more details. In all cases, a ‘swelling+ Ca^{2+} ’ stimulus was applied, and measurements were done after at least five minutes from the beginning of this stimulation. $N=11$

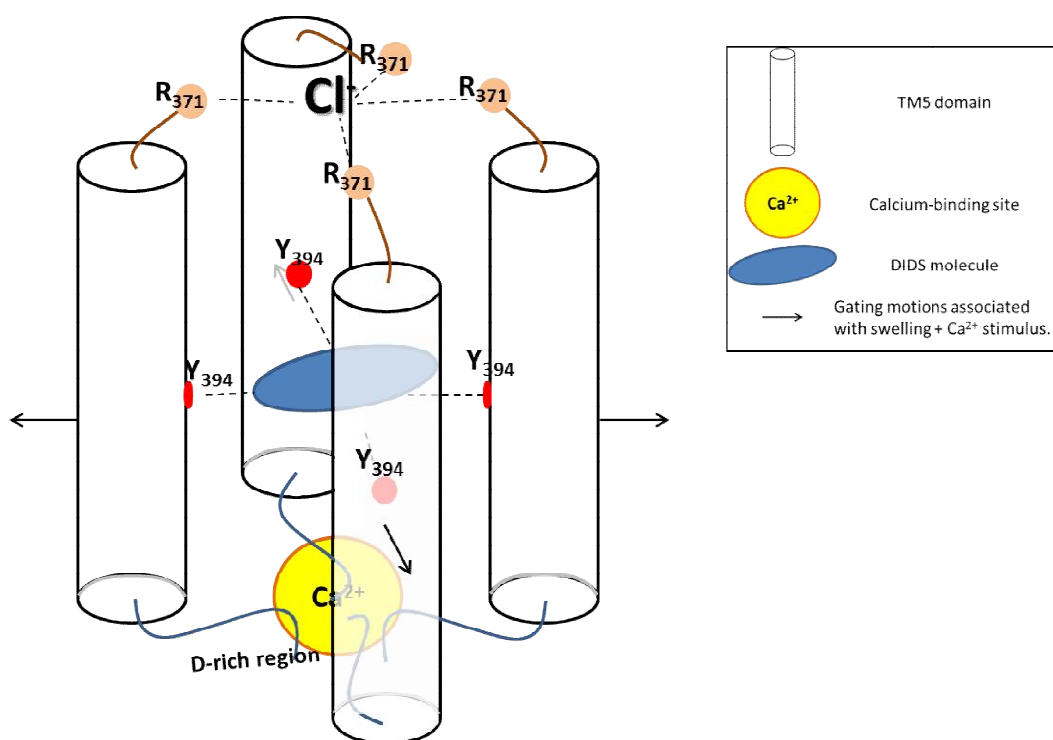


Fig. 5. Illustration summarizing the findings of our study

Only the pore of the channel is represented, with each TM5 domain of the tetramer contributing to the pore. Arginine 371 residues present in the loop between TM4 and TM5 may provide a positively-charged ring at the entrance of the pore, forming part of the selectivity filter of the channel. Past the carboxyl terminus of TM5, there is an Aspartate-rich region. These negative charges may contribute to a Ca^{2+} -binding site somewhat resembling the “ Ca^{2+} bowl” of BKCa channels. A tetrameric assembly together with an intracellular Ca^{2+} binding site, is similar to what is present in these potassium channels, and accordingly, it has been reported that calcium-activated chloride channels and BKCa share some pharmacological agents [26]. In hTTYH1 – unlike hTTYH3 – cell swelling instead of Ca^{2+} is the primary determinant of channel activation, but Ca^{2+} seems to assist in the gating process after that, suggesting that it is both swelling and Ca^{2+} sensitive (swelling influences are represented in the illustration by the arrows). Finally, DIDS has an electrical distance of block of 0.5, which approximately corresponds to the position of F394, half way across the membrane. Furthermore, the mutation F394S results in Kd values significantly higher, while the electrical distance remains unchanged, suggesting that DIDS binds within the pore in nearly the same position after the mutation, but the lack of the hydrophobic Phenylalanine results in much weaker binding. Thus, it is likely that even though F394 importantly contributes to DIDS binding at the blocking site, other residues also contribute, likely through hydrophobic interactions

The strategy of using a blocker to gain insight into the possible structure of the pore is one that we have used with success in the past [18,19]. Hence, with this strategy in mind, and guided by our model, we looked for a residue to mutate deep within the pore, which may further strengthen our conclusions so far. In TM5, a single Phenylalanine surrounded by Leucine residues half-way across the membrane, looked as a particularly good target for mutations, because it is facing the center of the pore, and because its aromatic ring may interact with the ones of the DIDS molecule, thus providing some scaffold for DIDS blockade. Indeed, we observed that the effect of the F394S mutation is

consistent with a scheme where DIDS binds F394 at an electrical distance within the pore of about 0.5. Replacement of Phenylalanine with Serine at that position, did not significantly change the electrical distance of blockade by DIDS, suggesting that other hydrophobic residues (several Leucine residues in the vicinity) may still provide a binding site for DIDS, yet with a lower affinity, as evidenced by the increased Kd value resulting from the mutation. Thus, these results indicate that interaction of DIDS with the side group of F394 is a relevant factor for stabilization of the binding site related to DIDS blockade (see Fig. 5 for a representation).

5. CONCLUSION

In summary, our results from the modeling approach allow to make suggestions about putatively important residues in channel function, and to verify them through a site-directed mutagenesis strategy, as it was the case in the present study. This same approach may be helpful for other membrane channel proteins with unknown structure.

ACKNOWLEDGEMENTS

This study counts with support from: C16-FAI-09-20.20, Fondo de Apoyo a la Investigación UASLP; PRODEP SEP Apoyo a la Incorporación de NPTC.

COMPETING INTERESTS

Authors have declared that no competing interests exist.

REFERENCES

- Moraes I, Evans G, Sanchez-Weatherby J, Newstead S, Stewart PDS. Membrane protein structure determination — The next generation. *Biochimica et Biophysica Acta (BBA) - Biomembranes*. 2014;1838(1, Part A):78-87.
- Fischer AW, Alexander NS, Woetzel N, Karakas M, Weiner BE, Meiler J. BCL::MP-fold: Membrane protein structure prediction guided by EPR restraints. *Proteins*. 2015; 83(11):1947-62.
- Koehler Leman J, Ulmschneider MB, Gray JJ. Computational modeling of membrane proteins. *Proteins*. 2015;83(1):1-24.
- Weiner Brian E, Woetzel N, Karakaş M, Alexander N, Meiler J. BCL::MP-Fold: Folding membrane proteins through assembly of transmembrane helices. *Structure*. 2013;21(7):1107-1117.
- Hopf TA, Schärfe CPI, Rodrigues JPGLM, Green AG, Kohlbacher O, Sander C, et al. Sequence co-evolution gives 3D contacts and structures of protein complexes. *eLife*. 2014;3:e03430.
- Halleran AD, Sehdev M, Rabe BA, Huyck RW, Williams CC, Saha MS. Characterization of tweety gene (ttyh1-3) expression in *Xenopus laevis* during embryonic development. *Gene Expression Patterns*. 2015;17(1):38-44.
- Suzuki M. The drosophilatweety family: molecular candidates for large-conductance Ca²⁺-activated Cl⁻ channels. *Experimental Physiology*. 2006;91(1):141-147.
- Suzuki M, Mizuno A. A novel human Cl⁻ channel family related to *Drosophila* flightless locus. *J Biol Chem*. 2004; 279(21):22461-8.
- Stefaniuk M, Swiech L, Dzwonek J, Lukasiuk K. Expression of Ttyh1, a member of the Tweety family in neurons *in vitro* and *in vivo* and its potential role in brain pathology. *Journal of Neurochemistry*. 2010;115(5):1183-1194.
- He Y, Ramsay AJ, Hunt ML, Whitbread AK, Myers SA, Hooper JD. N-glycosylation analysis of the human tweety family of putative chloride ion channels supports a penta-spanning membrane arrangement: Impact of N-glycosylation on cellular processing of tweety homologue 2 (TTYH2). *Biochem J*. 2008;412(1):45-55.
- Wiernasz E, Kaliszewska A, Brutkowski W, Bednarczyk J, Gorniak M, Kaza B, et al. Ttyh1 protein is expressed in glia *in vitro* and shows elevated expression in activated astrocytes following status epilepticus. *Neurochemical Research*. 2014;39(12):2516-2526.
- Morciano M, Beckhaus T, Karas M, Zimmermann H, Volkhardt W. The proteome of the presynaptic active zone: From docked synaptic vesicles to adhesion molecules and maxi-channels. *Journal of neurochemistry*. 2009;108(3):662-675.
- Rae FK, Hooper JD, Eyre HJ, Sutherland GR, Nicol DL, Clements JA. TTYH2, a human homologue of the *Drosophila melanogaster* gene tweety, is located on 17q24 and upregulated in renal cell carcinoma. *Genomics*. 2001;77(3):200-7.
- Toiyama Y, Mizoguchi A, Kimura K, Hiro J, Inoue Y, Tutumi T, et al. TTYH2, a human homologue of the *Drosophila melanogaster* gene tweety, is up-regulated in colon carcinoma and involved in cell proliferation and cell aggregation. *World J Gastroenterol*. 2007;13(19):2717-21.
- Deng L, Yang J, Chen H, Ma B, Pan K, Su C, et al. Knockdown of TMEM16A suppressed MAPK and inhibited cell proliferation and migration in hepatocellular carcinoma. *Onco Targets Ther*. 2016;9: 325-33.
- Jia L, Liu W, Guan L, Lu M, Wang K. Inhibition of calcium-activated chloride channel ANO1/TMEM16A suppresses

- tumor growth and invasion in human lung cancer. PLoS One. 2015;10(8):e0136584.
17. Duran C, Thompson CH, Xiao Q, Hartzell HC. Chloride channels: Often enigmatic, rarely predictable. *Annu Rev Physiol.* 2010;72:95-121.
 18. Reyes JP, Huanosta-Gutierrez A, Lopez-Rodriguez A, Martinez-Torres A. Study of permeation and blocker binding in TMEM16A calcium-activated chloride channels. *Channels (Austin).* 2015;9(2): 88-95.
 19. Reyes JP, Lopez-Rodriguez A, Espino-Saldana AE, Huanosta-Gutierrez A, Miledi R, Martinez-Torres A. Anion permeation in calcium-activated chloride channels formed by TMEM16A from *Xenopus tropicalis*. *Pflugers Arch.* 2014;466(9): 1769-77.
 20. Morcos F, Hwa T, Onuchic JN, Weigt M. Direct coupling analysis for protein contact prediction. *Methods Mol Biol.* 2014;1137: 55-70.
 21. Marks DS, Hopf TA, Sander C. Protein structure prediction from sequence variation. *Nat Biotechnol.* 2012;30(11): 1072-80.
 22. Hopf TA, Scharfe CP, Rodrigues JP, Green AG, Kohlbacher O, Sander C, et al. Sequence co-evolution gives 3D contacts and structures of protein complexes. *Elife.* 2014;3.
 23. Pierce BG, Wiehe K, Hwang H, Kim BH, Vreven T, Weng Z. ZDOCK server: Interactive docking prediction of protein-protein complexes and symmetric multimers. *Bioinformatics.* 2014;30(12): 1771-3.
 24. Woodhull AM. Ionic blockage of sodium channels in nerve. *The Journal of General Physiology.* 1973;61(6):687-708.
 25. Eilers M, Shekar SC, Shieh T, Smith SO, Fleming PJ. Internal packing of helical membrane proteins. *Proceedings of the National Academy of Sciences.* 2000; 97(11):5796-5801.
 26. Greenwood IA, Leblanc N. Overlapping pharmacology of Ca²⁺-activated Cl⁻ and K⁺ channels. *Trends in Pharmacological Sciences.* 2007;28(1):1-5.
 27. Yang H, Zhang G, Cui J. BK channels: Multiple sensors, one activation gate. *Frontiers in Physiology.* 2015;6:29.

© 2016 Reyes et al.; This is an Open Access article distributed under the terms of the Creative Commons Attribution License (<http://creativecommons.org/licenses/by/4.0>), which permits unrestricted use, distribution, and reproduction in any medium, provided the original work is properly cited.

Peer-review history:

The peer review history for this paper can be accessed here:
<http://sciedomain.org/review-history/16648>